Published in *Fluctuations and Noise in Biological, Biophysical and Biomedical Systems II*, eds. D. Abbott, S. M. Bezrukov, A. Der and A Sanchez, Proc. of SPIE vol. 5467, Bellingham, 2004, pp 192-201.

Resonant activation in single and coupled stochastic FitzHugh-Nagumo elements

Andrey V. Polovinkin[a], Evgeniya V. Pankratova[a],
Dmitry G. Luchinsky[b], Peter V.E. McClintock[b]

[a]Department of Radiophysics, Nizhny Novgorod State University,
Nizhny Novgorod, Gagarin Avenue 23, 603950 Russia.
[b]Department of Physics, Lancaster University, Lancaster LA1 4YB, UK.

ABSTRACT

The response of a noisy FitzHugh-Nagumo (FHN) neuron-like model to weak periodic forcing is analyzed. The mean activation time is investigated as a function of noise intensity and of the parameters of the external signal. It is shown by numerical simulation that there exists a frequency range within which the phenomenon of resonant activation occurs; resonant activation is also observed in coupled FHN elements. The mean activation time with small noise intensity is compared with the theoretical results.

Keywords: Resonant activation, weak periodic driving, mean activation time, coupled excitable systems, optimal paths.

1. INTRODUCTION

It is well known that living tissue, including nerve fibers in animals, is very sensitive to external forcing.[1–3] Furthermore, biological signal processing takes place in a fluctuating environment. So it is important, and of interest, to try to understand the statistical properties of stochastic neuronal systems and, in particular, to investigate the mutually cooperative influence of noise and external driving on the behaviour of the neurons. This is a problem that has been the subject of intensive research, both for single and coupled neuron-like elements.[4–12] One of the most intriguing phenomena, that of stochastic resonance,[13–15] has been observed in the case of simultaneous action of noise and weak (subthreshold) periodic driving on the system. It has been demonstrated that the response of neurons to the external driving can be optimized in this case by the presence of a particular level of noise. It has also been shown that noise can substantially modify the dynamical properties of the system even in the absence of external driving, leading to the occurrence of the well-known phenomenon of coherence resonance.[16–19] It can thus be seen, even from this brief description, that noise plays a significant role in optimization of the detection, transmission and encoding of signals in neurons.

Despite the broad interest of this problem, however, an understanding of the role of fluctuations in nerve cells still remains elusive, which is why investigation of the different parameter-dependent characteristics for both single neuron-like elements, and ensembles of them, in the presence of various external perturbations is of particular importance.

Recently very substantial progress has been made towards the understanding of fluctuation-induced escape from a metastable state, and of activated processes in general, by using the path-integral concept.[20–24] In the present paper we attempt to apply this technique for the examination of our numerical results. We examine the stochastic FitzHugh-Nagumo (FHN) model in the presence of weak periodic forcing with the aim of shedding new light on the response of neurons to an external signal in the presence of noise. We will investigate the mean activation time in a single FHN element (section 3) and two coupled elements (section 4) as functions of noise intensity and of the parameters of the external periodic signal. It will be demonstrated that resonant activation[25–27] occurs in both cases. For coupled units, the influence of the coupling factor on this effect will be illustrated. The mean activation time found in numerical experiments will be compared with the theoretical prediction.

Correspondence to Andrey V. Polovinkin: E-mail polovinkin@rf.unn.ru; Telephone: +7 (8312) 656 242

2. MODEL AND METHODS OF INVESTIGATION

We consider the following FHN neuron-like model:

$$\begin{aligned} \dot{x} &= F_1(x,y) + A\sin(\omega t) = x - x^3/3 - y + A\sin(\omega t) \\ \dot{y} &= F_2(x,y) + \xi(t) = \varepsilon(x + I) + \xi(t), \end{aligned} \tag{1}$$

where: $\xi(t)$ is white Gaussian noise with correlation function $\langle \xi(t)\xi(t+\tau)\rangle = D\delta(\tau)$; and ε and I are the system parameters ($\varepsilon = 0.05$ is a small parameter, and $I = 1.05$). The curve $F_1(x,y) = 0$ has an N-like form, while $F_2(x,y) = 0$ is a straight line. In the absence of both external driving and noise there is only one steady state of the system (1) corresponding to the point of intersection $A(x^0, y^0)$ of the curves $F_1(x,y) = 0$ and $F_2(x,y) = 0$ in the zero-noise limit. It has coordinates $x^0 = -I, y^0 = -I + I^3/3$. In this perturbation-free case all trajectories of the system (1) will be attracted to $A(x^0, y^0)$. In our simulations we assumed that the voltage-like variable x is subjected to a subthreshold periodic drive of amplitude A and circular frequency ω. Subthreshold driving means that the external signal alone is not of sufficient amplitude to produce a response from the neuron (i.e., to generate a spike).

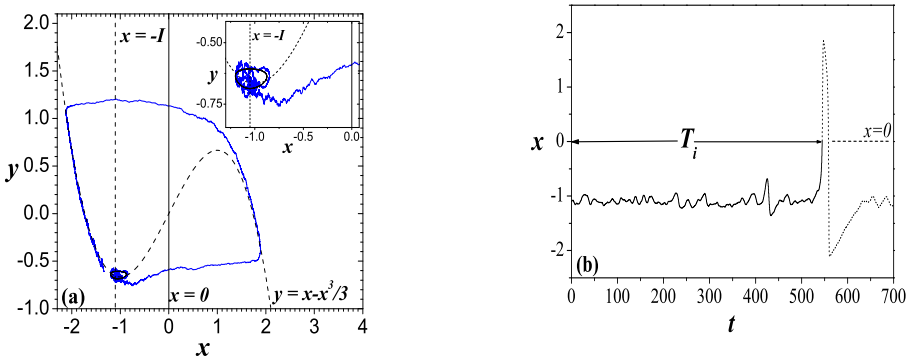

Figure 1. (a) Phase diagram for the system (1). Dashed lines correspond to nullclines of the unperturbed deterministic case: $x = -I$ and $y = x - x^3/3$. The deterministic stable ellipse-like curve is shown by the solid closed line. An enlarged version of the phase diagram in the vicinity of the stable state is shown in the inset. (b) An example of a stochastic trajectory of the system (1). The activation time T_i is calculated as the time to the first crossing of the boundary $x = 0$ as shown in the figure.

Subthreshold periodic driving in the absence of noise leads to the establishment of periodic motion in the configuration space $\{\mathbf{x}, t\}$ whose projection on the plane $\{\mathbf{x}\} = \{x, y\}$ looks like a limit cycle: see inset of Fig. 1(a).

2.1. Numerical simulation

The presence of noise leads to the generation of a response in the system. Our numerical simulations are based on a noise generator producing Gaussian, normally distributed, deviations of zero mean and unit variance, and we use a modified midpoint method[28] for the integration of (1). We will focus on one of the characteristic time scales, choosing that known as the mean activation time. It is obtained as the average of first passage times across the boundary $x = 0$:

$$T = \frac{1}{N}\sum_{i=1}^{N} T_i, \tag{2}$$

where T_i is the activation time for i-th realization, Fig. 1(b).

2.2. Path-integral based technique for obtaining the mean activation time

It is known that many statistical characteristics of stochastic motion for the system (1) can be obtained by making use of the Fokker-Plank equation (FPE)[29]:

$$\partial_t \rho(\mathbf{x},t) = -\tfrac{1}{2} D \partial_i \partial_j [Q^{ij} \rho(\mathbf{x},t)] + \partial_i [F_i(\mathbf{x},t) \rho(\mathbf{x},t)], \tag{3}$$

where: the notation means $\partial_t = \frac{\partial}{\partial t}, \partial_i = \frac{\partial}{\partial x_i}, \partial_i \partial_j = \frac{\partial^2}{\partial x_i \partial x_j}$; $\rho(\mathbf{x},t)$ is the probability density which completely specifies the system dynamics in the presence of noise; $\mathrm{Q} = (Q^{ij})$ is the diffusion matrix, whose elements are $Q^{22} = 1$, $Q^{ij} = 0$ for $i \neq 2$ or $j \neq 2$, in our simulation. F_i are the right-hand deterministic parts of the Langevin equations (1): $F_1 = x - x^3/3 - y + A\sin(\omega t)$, $F_2 = \varepsilon(x + I)$.

In the small-noise limit, the probability density $\rho(\mathbf{x},t)$ of the stochastic process $\mathbf{x}(t)$ can be written in the WKB-like approximate form[30,31]:

$$\rho(\mathbf{x},t) \sim \mathcal{Z}(\mathbf{x},t) \exp\{-S(\mathbf{x},t)/D\}, \tag{4}$$

where $\mathcal{Z}(\mathbf{x},t)$ is a prefactor, and the action function $S(\mathbf{x},t)$ plays the role of a non-equilibrium potential.[32] Substituting Eq. (4) into the FPE (3), and expanding in powers of D, allows one to obtain the equations for the action and prefactor[30,31,33–35] in the leading and next-to-leading orders of approximation. It follows from this expansion that the function $S(\mathbf{x},t)$ satisfies the Hamilton-Jacobi equation for a classical action of form:

$$\partial_t S(\mathbf{x},t) + H(\mathbf{x}, \nabla S) = 0, \tag{5}$$

where $H(x_i, p_i) = \frac{1}{2} Q^{ij} p_i p_j + F_i(\mathbf{x},t) p_i$ is the Hamiltonian function that must be chosen equal to zero to provide a proper description of exponentially slow escape from the metastable state.[34] This suggests a classical mechanical interpretation of the function $S(\mathbf{x},t)$ and allows one to calculate it as an action integral taken along the trajectories of an *auxiliary* Hamiltonian system. The corresponding Hamilton's equations take the form:

$$\begin{aligned} \dot{x}_i &= F_i(\mathbf{x},t) + Q^{ij} p_j \\ \dot{p}_i &= -p_j \partial_i F_j. \end{aligned} \tag{6}$$

These equations must be solved simultaneously with the equations for the action function and prefactor in the form[30]:

$$\dot{S}(\mathbf{x},t) = p_i \dot{x}_i - H = p_i [F_i(\mathbf{x},t) + Q^{ij} p_j], \tag{7}$$

$$\dot{\mathcal{Z}}(\mathbf{x},t) = -\left[\frac{1}{2} Q^{ij} \partial_i \partial_j S(\mathbf{x},t) + \partial_i F_i(\mathbf{x},t) \right] \mathcal{Z}(\mathbf{x},t) \tag{8}$$

We note that the equation for the prefactor (8) involves an unknown Hessian matrix ($S_{,ij} \equiv \partial_i \partial_j S$). The system of equations (6)-(8) must therefore be closed by adding an equation for the time evolution of the Hessian matrix itself. The latter can be obtained[34] by differentiation of the Hamilton-Jacobi equation with respect to position and momentum along the trajectories of (6):

$$\dot{S}_{,ij} = -Q^{yy} S_{,iy} S_{,jy} - \frac{\partial^2 H}{\partial x_j \partial p_k} S_{,ik} - \frac{\partial^2 H}{\partial x_i \partial p_k} S_{,jk} - \partial_i \partial_j H \tag{9}$$

Finally, simultaneous integration of the system of coupled ordinary differential equations (6)-(9) allows one to calculate the action function and prefactor, and hence the probability density (4). To obtain the mean first passage time (MFPT) let us rewrite the FPE (3) in the following form:

$$\partial_t \rho(\mathbf{x},t) = -\mathrm{div}\mathbf{G}, \tag{10}$$

where

$$\mathbf{G} = -\tfrac{1}{2} D \mathrm{grad}(\mathrm{Q}\,\rho(\mathbf{x},t)) - \mathbf{F}(\mathbf{x},t) \rho(\mathbf{x},t) \tag{11}$$

is the probability density current. The MFPT of escape from the basin of attraction Ω of a metastable state A of the system (1) via the basin boundary $\partial\Omega$ is thus given by the following formula[29, 36]:

$$T = \frac{\int\limits_{\Omega} \rho(\mathbf{x}, t) d\mathbf{x}}{\int\limits_{\partial\Omega} (\mathbf{G}, \mathbf{n})\, d(\partial\Omega)} \tag{12}$$

where $\mathbf{n}$ is the vector of the unit outer normal for the basin of attraction Ω. Thus, knowing the current values (i.e. the probability density) on the boundary $\partial\Omega$ allows us to obtain the mean activation time.

The separatrix $\partial\Omega$ is a solution of (1) in the absence of noise, separating the deterministic trajectories that are attracted to the right and left-hand stable branches of the slow-motion curve $y = x - x^3/3$ (Fig. 2).

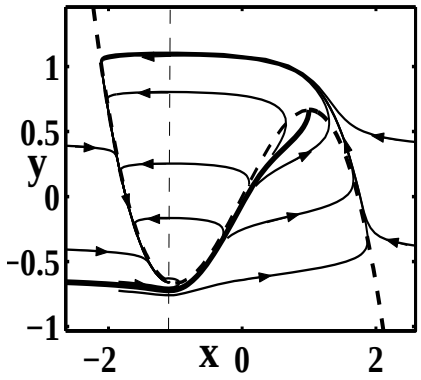

Figure 2. Phase portrait of the system (1) in the absence of noise. Dashed lines correspond to the nullclines as explained in Fig. 1. The separatrix is shown by the bold solid line. Deterministic trajectories of the system are shown by the solid lines with arrows.

In what follows we assume that the separatrix does not change in the presence of external driving. This is a strong assumption that will be analyzed in more detail elsewhere.

2.2.1. Without periodic driving

Let us now analyze in detail the integral in the denominator of the (12). In what follows this integral will be denoted as $\mathcal{J}$. We note that, in our particular case, the separatrix $\partial\Omega$ is defined by the condition $(\mathbf{n}, \mathbf{F}) = 0$. Taking this into account, the integral $\mathcal{J}$ can be rewritten as:

$$\mathcal{J} = \frac{1}{2} \int\limits_{\partial\Omega} \left[\frac{D}{\mathcal{Z}} \frac{\partial \mathcal{Z}}{\partial y} - p_y \right] \exp\{-S_{mod}/D\} (\mathbf{n}, \mathbf{e}_y) dl(x) \tag{13}$$

where $\mathbf{e}_y$ is a unit vector in the y-direction. The integration in (13) is taken along the separatrix. $S_{mod} = S - D \ln \mathcal{Z}$ is a modified action function.

It can be seen from Fig. 3(a) that S_{mod} is a non-monotonic function of position on the separatrix and has minimum at $x = x_{min}$. The integral $\mathcal{J}$ we can calculate numerically over the whole separatrix.[35] However, for investigation of the effect of periodic driving a more detailed analysis is required. Therefore, we evaluate the integral (13) using a steepest descent technique, expanding the modified action function in Taylor series in a small vicinity of the point x_{min}:

$$\mathcal{J} = \left[\frac{1}{2} \left(\frac{D}{\mathcal{Z}} \frac{\partial \mathcal{Z}}{\partial y} - p_y \right) \exp\{-S_{mod}/D\} \sqrt{\frac{2\pi D}{S''_{mod_{xx}}}} \right]_{x = x_{min}} . \tag{14}$$

The results of these calculations are compared with numerical simulations in Fig. 3(b).

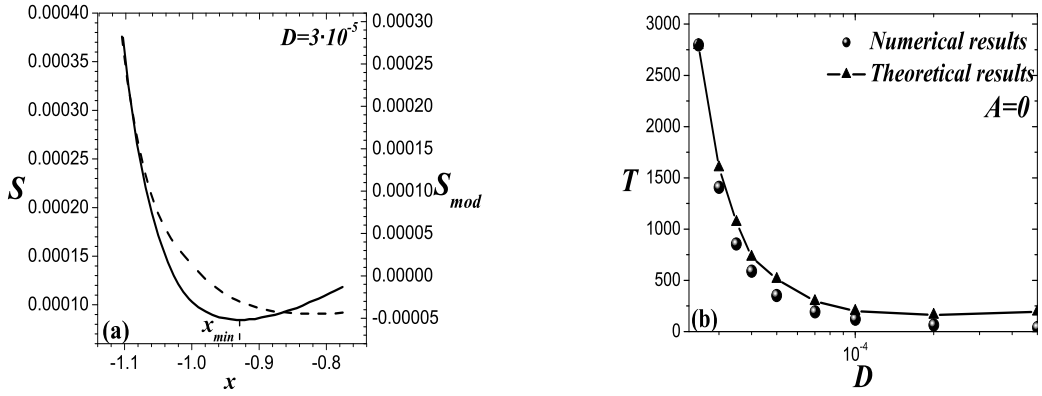

Figure 3. (a) Action function (dashed line) and modified action function (solid line) as a function of the variable x (without periodic driving); (b) The MFPTs found in the numerical simulations (filled dots) are compared with theoretical predictions based on Eq. (14) (triangles).

3. INFLUENCE OF SUBTHRESHOLD DRIVING ON THE MEAN ACTIVATION TIME FOR A SINGLE FHN ELEMENT

In the presence of noise, the additional subthreshold periodic driving can induce a substantial decrease of the mean activation time T, Fig. 4(a). Furthermore, there exists an optimal frequency for which the MFPT takes a minimum value, corresponding to the phenomenon of resonant activation.[37]

The results obtained by numerical investigation of resonant activation in our system are summarized in Fig. 4. It can be seen that a change in the amplitude of the external driving has a pronounced effect on the escape rates. Fig. 4(a) shows a deepening and broadening of the resonance curve as the amplitude A of the drive is increased.

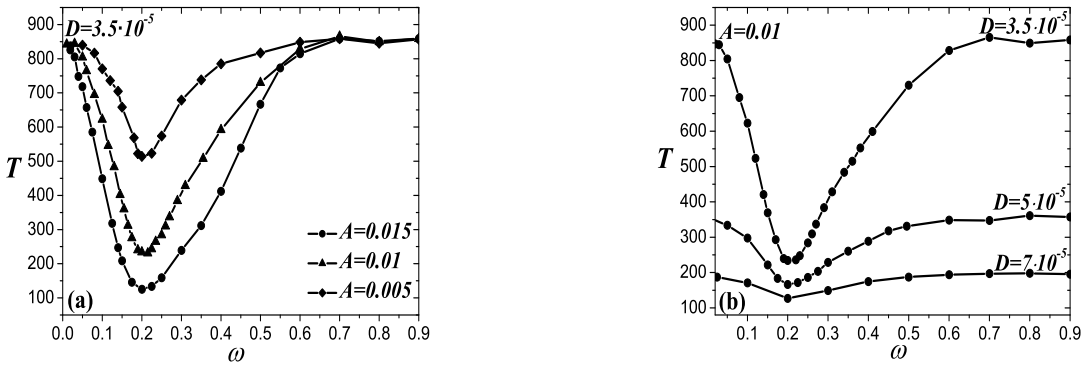

Figure 4. Numerical calculations of the mean activation time as a function of driving frequency: (a) for different amplitudes of the external signal with $D = 3.5 \cdot 10^{-5}$; and (b) for different noise intensities with $A = 0.01$.

3.1. Theoretical analysis considering the influence of periodic driving

Periodically driven nonlinear oscillators under non-adiabatic conditions in the presence of noise were analyzed by Dykman and Smelyansky.[38] In our present studies we try to adapt their technique to the analysis of the non-adiabatic driving of excitable systems. We therefore assume[38,39] that the dominant effect of resonant activation

is a field-induced variation of the action function. This is of course a simple consequence of the fact that the effect of varying the action is exponentially strong. It is also clear that the smaller the noise intensity is, the better becomes the corresponding approximation function, since the action in the exponent is divided by the small parameter D. It is also important to bear in mind that the approximation suggested by Dykman et al[38, 39] is valid only in the region of parameters where the change in the action function is linearly proportional to the change in the amplitude of the driving force. Finally, we note that we have adopted in this paper the next-to-leading order of the WKB-approximation. The latter requires that the noise-induced changes of the action must be much smaller then the value of action in the zero-noise limit. Having in mind the above restrictions we proceed as follows. The Hamilton's equations of motion of the auxiliary Hamiltonian system for a singled out stochastic FHN model (1) take the following form:

$$\begin{cases} \dot{x} = F_1 + Q^{i1}p_i = x - x^3/3 - y + A\sin(\omega t + \varphi_0), \\ \dot{y} = F_2 + Q^{j2}p_j = \epsilon(x + I) + p_y, \\ \dot{p}_x = -(1 - x^2)p_x - \epsilon p_y, \\ \dot{p}_y = p_x. \end{cases} \tag{15}$$

Correspondingly, equations (7), (8), and (9) take the form:

$$\begin{cases} \dot{S} = [x - x^3/3 - y + A\sin(\omega t + \varphi_0)]p_x + [\epsilon(x + I) + p_y]p_y, \\ \dot{\mathcal{Z}} = -[\frac{1}{2}S_{,yy} + (1 - x^2)]\mathcal{Z}, \\ \dot{S}_{,ij} = -\frac{1}{2}S_{,iy}S_{,jy} - \frac{\partial F_k}{\partial x_j}S_{,ik} - \frac{\partial F_k}{\partial x_i}S_{,jk} + 2xp_x^2\delta_{i1}\delta_{j1}, \end{cases} \tag{16}$$

where $i, j, k = x, y$.

To describe the initial conditions, we linearize[34, 40, 41] equations (15) near the stable point A in the absence of the driving force to obtain:

$$\begin{cases} \delta\dot{x} = (1 - I^2)\delta x - \delta y, \\ \delta\dot{y} = \epsilon\delta x + p_y, \\ \dot{p}_x = -(1 - I^2)p_x - \epsilon p_y, \\ \dot{p}_y = p_x. \end{cases} \tag{17}$$

A generic point on the unstable manifold is written in this case as $v(t) = \alpha_1 v_1^u \exp^{\lambda_1 t} + \alpha_2 v_2^u \exp^{\lambda_2 t}$ where $\alpha_{1,2}$ are complex coefficients and λ_1 and λ_2 are two positive eigenvalues corresponding to the unstable eigenvectors v_1^u and v_2^u. Accordingly, the connection between the momenta and coordinates on the unstable manifold of the linearized system can be written as:

$$\begin{pmatrix} p_x \\ p_y \end{pmatrix} = \mathcal{M}\begin{pmatrix} x \\ y \end{pmatrix}, \quad \text{where} \quad \mathcal{M} = \begin{pmatrix} v_{1p_x} & v_{2p_x} \\ v_{1p_y} & v_{2p_y} \end{pmatrix}\begin{pmatrix} v_{1x} & v_{2x} \\ v_{1y} & v_{2y} \end{pmatrix}^{-1}. \tag{18}$$

Equations (18) provide the choice of proper initial conditions for the integration of equations (6)–(9). Indeed, in the vicinity of the stable point (x^0, y^0), the action can be approximated in the form $S(\mathbf{x}) = \frac{1}{2}\mathbf{x}^T\mathcal{M}\mathbf{x}$. The matrix $\mathcal{M}$ therefore defines the curvature of the action surface in the vicinity of the stable state and the prefactor according to the approximation (4).

An iterative analysis of (16) shows that the variation of action $\delta S(\omega, \varphi_0)$ takes the form:

$$\delta S(\omega, \varphi_0) = A\mathcal{W} + \mathcal{O}(A^2), \tag{19}$$

where $\delta S(\omega, \varphi_0)$ is the correction to the action $S|_{A=0}$ that was obtained without periodic driving in the limit of zero noise intensity; $\mathcal{W}$ is the work done by a unit force along the optimal trajectory of the unperturbed system (6).

For finite noise intensity, we adopt a similar approximation but with the following modifications. The role of the most probable escape path is taken by the path that provides a minimum of the modified action at the boundary at $x = x_{min}$, and the upper limit of integration is not finite but, rather, is defined by the condition that the modified most probable escape path crosses the boundary.

Consequently, the integral in the denominator of (12) must be averaged over one period of the external driving, and will take the following form:

$$\mathcal{J} = \left[\frac{1}{4\pi}\left(\frac{D}{\mathcal{Z}}\frac{\partial \mathcal{Z}}{\partial y} - p_y\right)\exp\{-S_{mod}/D\}\sqrt{\frac{2\pi D}{S''_{mod_{xx}}}}\right]_{x=x_{min}} \int \exp\{-\delta S(\omega,\varphi_0)/D\}d\varphi_0 \tag{20}$$

These theoretical results for the mean activation time are compared with the results of numerical simulation in Fig. 5. It should be mentioned here that, the smaller the noise intensity D, the bigger becomes the

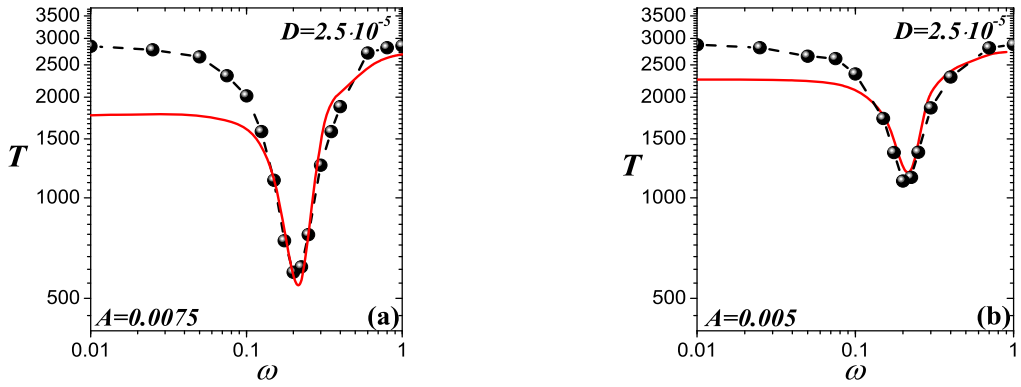

Figure 5. Mean activation time as a function of the frequency of the periodic signal. The theoretical results (solid lines) are compared with numerical calculations (circles) for $D = 2.5 \cdot 10^{-5}$ with: (a) $A = 0.0075$; and (b) $A = 0.005$.

relative decrease of the mean activation time, Fig. 4(b). This occurs because the pre-exponential factor in $\frac{1}{2\pi D}\int \exp\{-\delta S(\omega,\varphi_0)\}d\varphi_0$ is inversely proportional to D.

4. INFLUENCE OF SUBTHRESHOLD DRIVING ON THE MEAN ACTIVATION TIME FOR TWO COUPLED FHN ELEMENTS

In this section we consider co-operative dynamics in a system of two coupled FHN elements:

$$\begin{aligned}
\dot{x}_1 &= x_1 - x_1^3/3 - y_1 + A\sin(\omega t) + p(x_2 - x_1),\\
\dot{y}_1 &= \varepsilon(x_1 + I_1) + \xi_1(t),\\
\dot{x}_2 &= x_2 - x_2^3/3 - y_2 + A\sin(\omega t) + p(x_1 - x_2),\\
\dot{y}_2 &= \varepsilon(x_2 + I_2) + \xi_2(t),
\end{aligned} \tag{21}$$

where I_i are parameters of the partial element; p is the coupling coefficient; $\xi_{1,2}(t)$ are the independent components of a two-dimensional Gaussian white noise with correlation functions $\langle \xi_i(0)\xi_j(t)\rangle = D\delta_{ij}\delta(t)$. Further, the dependence of the mean activation time on the driving frequency was investigated for cases when both elements have identical initial conditions $I_1 = I_2 = 1.05$ (Fig. 6(a)), and $I_1 = I_2 = 1.1$ (Fig. 6(b)).

As we can see from Fig. 6, different tendencies exist here for the influence of coupling strength on the mean activation time for periodically and noisily perturbed FHN-elements. The activation of one element for subthreshold driving leads to a decrease of the mean activation time T for the second (non-activated) element. But if both elements are non-activated, and the response to the driving force is small, the mean activation time T of each element is increased due to the coupling because, for large coupling strength, fluctuational forcing of both elements must be correlated to procure their synchronized activation. The tendency for decreasing T is stronger with weak coupling strength when close to the bifurcation point where $I = 1$, Fig. 6(a). The tendency for increasing T is stronger for strong coupling or far from bifurcation point, Fig. 6(a,b). It is interesting to note that, while strong coupling hampers activation for all frequencies (Fig. 6(a),(b)), there exists a region in

parameter space where weak coupling leads to an increased activation rate for certain frequencies of external forcing near the resonant frequency and, on the contrary, to an increased mean activation time for frequencies of external forcing that are far from resonance ($p = 0.1$ on Fig. 6(b)).

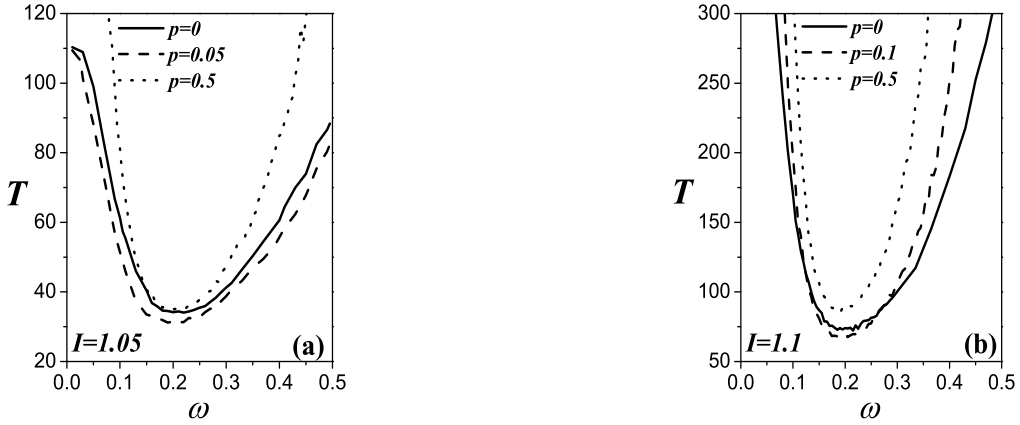

Figure 6. Activation time as a function of the frequency of external periodic forcing for various coupling strengths p in the cases of: (a) $I = 1.05$ for both elements; and (b) $I = 1.1$ for both elements.

Acknowledgments

The work was supported by the Engineering and Physical Research Council (UK), by INTAS (project N 01-8667), and by RFBR (project NN 03-02-17543).

REFERENCES

1. J. A. White, J. T. Rubinstein, and A. R. Kay, "Channel noise in neurons," *Trends Neurosci.* **23**(3), pp. 131–137, 2000.
2. E. R. Kandel, J. H. Schwartz, and T. M. E. Jessell, *Principles of Neural Science*, Appleton & Lange, Norwalk, 1991.
3. F. Moss and P. Xing, "Stochastic resonance – neurons in parallel," *Nature* **376**(6537), pp. 211–212, 1995.
4. V. Hakim and W. J. Rappel, "Noise-induced periodic behaviour in the globally coupled complex Ginzburg-Landau equation," *Europhys. Lett.* **27**(9), pp. 637–642, 1994.
5. A. Neiman, "Synchronization like phenomena in coupled stochastic bistable systems," *Phys. Rev. E* **49**(4), pp. 3484–3487, 1994.
6. B. Shulgin, A. Neiman, and V. Anishchenko, "Mean switching frequency locking in stochastic bistable systems driven by a periodic force," *Phys. Rev. Lett* **75**(23), pp. 4157–4160, 1995.
7. C. Kurrer and K. Schulten, "Noise-induced synchronous neuronal oscillations," *Phys. Rev. E* **51**(6), pp. 6213–6218, 1995.
8. J. F. Lindner, B. K. Meadows, W. L. Ditto, M. E. Inchiosa, and A. R. Bulsara, "Scaling laws for spatiotemporal synchronization and array enhanced stochastic resonance," *Phys. Rev. E* **53**(3), pp. 2018–2086, 1996.
9. J. M. G. Vilar and J. M. Rubi, "Divergent signal-to-noise ratio and stochastic resonance in monostable systems," *Phys. Rev. Lett.* **77**(14), pp. 2863–2866, 1996.
10. F. Marchesoni, L. Gammaitoni, and A. R. Bulsara, "Spatiotemporal stochastic resonance in a phi(4) model of kink-antikink nucleation," *Phys. Rev. Lett.* **76**(15), pp. 2609–2612, 1996.
11. P. Jung and G. Mayer-Kress, "Spatiotemporal stochastic resonance in excitable media," *Phys. Rev. Lett* **76**(11), pp. 2130–2133, 1995.

12. M. A. Santos and J. M. Sancho, "Noise-induced fronts," *Phys. Rev. E* **59**(1), pp. 98–102, 1999.
13. R. Benzi, A. Sutera, and A. Vulpiani, "The mechanism of stochastic resonance," *J. Phys. A* **14**(11), pp. L453–L457, 1981.
14. M. I. Dykman, D. G. Luchinsky, R. Mannella, P. V. E. McClintock, N. D. Stein, and N. G. Stocks, "Stochastic resonance in perspective," *Nuovo Cimento D* **17**(7–8), pp. 661–683, 1995.
15. L. Gammaitoni, P. Hänggi, P. Jung, and F. Marchesoni, "Stochastic resonance," *Rev. Mod. Phys.* **70**(1), pp. 223–287, 1998.
16. A. Pikovsky and J. Kurths, "Coherence resonance in a noise-driven excitable system," *Phys. Rev. Lett* **78**(5), pp. 775–778, 1997.
17. B. Hu and C. Zhou, "Synchronization regimes in coupled noisy excitable systems," *Phys. Rev. E* **63**(2), pp. 0262011–0262016, 2001.
18. S. R. Massanes and C. J. Perez Vicente, "Nonadiabatic resonances in a noisy FitzHugh-Nagumo model," *Phys. Rev. E* **59**(4), pp. 4490–4497, 1999.
19. B. Lindner and L. Schimansky-Geier, "Analytical approach to the stochastic FitzHugh-Nagumo system and coherence resonance," *Phys. Rev. E* **60**(6), pp. 7270–7276, 1999.
20. V. N. Smelyanskiy, M. I. Dykman, and B. Golding, "Time oscillations of escape rates in periodically driven systems," *Phys. Rev. Lett.* **82**(16), pp. 3193–3197, 1999.
21. V. N. Smelyanskiy, M. I. Dykman, H. Rabitz, B. E. Vugmeister, S. L. Bernasek, and A. B. Bocarsly, "Nucleation in periodically driven electrochemical systems," *J Chem. Phys.* **110**(23), pp. 11488–11504, 1999.
22. M. Arrayas, I. A. Khovanov, D. G. Luchinsky, R. Mannella, P. V. E. McClintock, M. Greenall, and H. Sabbagh, "Experimental studies of the non-adiabatic escape problem," in *Stochastic and Chaotic Dynamics in the Lakes*, D. S. Broomhead, E. A. Luchinskaya, P. V. E. McClintock, and T. Mullin, eds., pp. 20–25, American Institute of Physics, (Melville), 2000.
23. J. Lehmann, P. Reimann, and P. Hänggi, "Surmounting oscillating barrier," *Phys. Rev. Lett.* **84**(8), pp. 1639–1642, 2000.
24. R. S. Maier and D. L. Stein, "Noise-activated escape from a sloshing potential well," *Phys. Rev. Lett.* **86**(18), pp. 3942–3945, 2001.
25. C. R. Doering and J. C. Gadoua, "Resonant activation over a fluctuating barrier," *Phys. Rev. Lett.* **69**(16), pp. 2318–2321, 1992.
26. A. L. Pankratov and M. Salerno, "Resonant activation in overdamped systems with noise subjected to strong periodic driving," *Phys. Lett. A* **273**(3), pp. 162–166, 2000.
27. A. N. Malakhov and A. L. Pankratov, "Evolution times of probability distributions and averages – exact solutions of the Kramers' problem," *Adv. Chem. Phys.* **121**, pp. 357–438, 2002.
28. W. H. Press, B. P. Flannery, S. A. Teukolsky, and W. T. Vetterling, *Numerical Recipes in C*, Cambridge University Press, Cambridge, 1993.
29. H. Risken, *The Fokker-Plank Equation*, Springer, Berlin, 3rd ed., 1996.
30. D. Ludwig, "Persistence of dynamical systems under random perturbations," *SIAM Rev.* **17**(4), pp. 605–640, 1975.
31. M. Freidlin and A. D. Wentzel, *Random Perturbations in Dynamical Systems*, Springer, New-York, 1984.
32. R. Graham and T. Tel, "Existence of a potential for dissipative dynamical systems," *Phys. Rev. Lett.* **52**, pp. 9–12, 1984.
33. R. Graham, "Macroscopic potentials, bifurcation and noise in dissipative systems," in *Noise in Nonlinear Dynamical Systems*, volume I, F. Moss and P. V. E. McClintock, eds., pp. 225–278, Cambridge University Press, Cambridge, 1989.
34. R. S. Maier and D. L. Stein, "Limiting exit location distributions in the stochastic exit problem," *SIAM J. Appl. Math.* **57**(3), pp. 752–790, 1997.
35. D. G. Luchinsky, P. V. E. McClintock, A. Polovinkin, and G. V. Osipov, "Stochastic excitation and synchronization in coupled FitzHugh-Nagumo elements," in *Noise in Complex Systems and Stochastic Dynamics*, L. Schimansky-Geier, D. Abbott, A. Neiman, and C. van den Broeck, eds., pp. 301–308, SPIE, (Washington), June 2003.

36. R. S. Maier and D. L. Stein, "A scaling theory of bifurcations in the symmetrical weak-noise escape problem," *J. Stat. Phys.* **83**, pp. 291–357, 1996.
37. B. I. Ivlev and V. I. Mel'nikov, "Effect of resonant pumping on activated decay rates," *Phys. Lett. A* **116**, pp. 427–428, 1986.
38. M. I. Dykman, H. Rabitz, V. N. Smelyanskiy, and B. E. Vugmeister, "Resonant directed diffusion in nonadiabatically driven systems," *Phys. Rev. Lett.* **79**(7), pp. 1178–1181, 1997.
39. V. N. Smelyanskiy, M. I. Dykman, H. Rabitz, and B. E. Vugmeister, "Fluctuations, escape, and nucleation in driven systems: logarithmic susceptibility," *Phys. Rev. Lett.* **79**(17), pp. 3113–3116, 1997.
40. M. I. Dykman, "Large fluctuations and fluctuational transitions in systems driven by colored Gaussian noise: A high frequency noise," *Phys. Rev. A* **42**(4), pp. 2020–2029, 1990.
41. V. N. Smelyanskiy, M. I. Dykman, and R. S. Maier, "Topological features of large fluctuations to the interior of a limit cycle," *Phys. Rev. E* **55**(3), pp. 2369–2391, 1997.